Graphene mode-locked femtosecond Cr:ZnSe laser at 2500 nm

M. N. Cizmeciyan,[1,2] J. W. Kim,[3] S. Bae,[4] B. H. Hong,[4] F. Rotermund,[3,5] and A. Sennaroglu[1,2,6]

[1]*Laser Research Laboratory, Department of Physics, Koç University, Rumelifeneri, Sariyer, Istanbul 34450, Turkey*

[2]*Koç University Surface Science and Technology Center (KUYTAM), Rumelifeneri, Sariyer, Istanbul 34450, Turkey*

[3]*Department of Physics & Division of Energy Systems Research, Ajou University, Suwon 443-749, South Korea*

[4]*Department of Chemistry, Seoul National University, Seoul 151-747, South Korea*

[5]*e-mail: rotermun@ajou.ac.kr*

[6]*e-mail: asennar@ku.edu.tr*

Received November 19, 2012; accepted December 11, 2012;
posted January 3, 2013 (Doc. ID 180236); published January 28, 2013

We report, for the first time to our knowledge, femtosecond pulse generation from a graphene mode-locked Cr:ZnSe laser at 2500 nm. To minimize the insertion losses at the lasing wavelength, high-quality monolayer graphene transferred on a CaF_2 substrate was used in the experiments. Once mode-locking was initiated, the laser generated a stable train of 226 fs pulses with a time–bandwidth product of 0.39. The mode-locked laser operated at a pulse repetition rate of 77 MHz and produced 80 mW output power with an incident pump power of 1.6 W. To our knowledge, this is the longest laser wavelength at which graphene-based passive mode-locking has been demonstrated to date. © 2013 Optical Society of America

OCIS codes: 320.7090, 140.5680, 140.4050, 160.4330.

Recently there has been a great deal of interest in the development of robust modulators that can be used in the mode-locking of femtosecond solid-state lasers over a broad spectral range. The more conventionally used semiconductor saturable absorber mirrors (SESAMs) have the drawback of operating only over a limited wavelength range set by the resonant behavior of the semiconductor quantum well structure and the bandwidth of the high-reflector coating [1]. To overcome the operation bandwidth and tuning range limitations, single-walled carbon nanotube saturable absorbers (SWCNT-SAs) and graphene saturable absorbers (GSAs) have been used [2,3]. With SWCNT-SAs, mode-locked operation in the wavelength range of 800–2070 nm has been demonstrated [4,5]. Use of SWCNT-SAs at longer wavelengths is limited due to the infrared absorption of the polymethyl methacrylate (PMMA) host. Furthermore, practical limits in the diameter of currently producible single-walled carbon nanotubes have kept the corresponding transition wavelengths of the SWCNT-SAs near or below 2 μm [5].

In comparison with SESAMs and SWCNT-SAs, GSAs offer the great potential of overcoming the spectral limitations discussed above. This is because even a single atomic layer of graphene, possessing a point-bandgap structure, has been shown to provide sufficient saturable absorption over an ultrawide range of wavelengths. Furthermore, no additional polymer matrix is required to hold the saturable absorber on the substrate. In this case, the absorption band resulting from graphene extends from the visible to the infrared with a constant value of $\pi\alpha$, where α is the fine structure constant given by $1/137$. To date, many fiber [6] and solid-state lasers [7–9] have been mode-locked by utilizing graphene as a saturable absorber in a broad wavelength range. Among them, the longest achieved mode-locked operation wavelength was near 2 μm [9].

The remaining challenge in extending the operation wavelength of GSAs is to improve the transparency range of the substrate. This is especially a problem with the commonly used quartz substrates beyond 2 μm [10,11] and can be remedied by using infrared-transparent substrates such as calcium fluoride (CaF_2). GSAs that can be effectively employed in the mid-infrared are crucial in the development of stable, mid-infrared femtosecond sources that are needed in numerous emerging applications, including high-precision dual comb spectroscopy, pumping of optical parametric oscillators at higher wavelengths, and efficient generation of high harmonics [12,13]. A suitable candidate to test the applicability of these saturable absorbers beyond 2 μm is the Cr:ZnSe laser, which can provide broadly tunable radiation from 1880 to 3349 nm [14,15]. In addition, since the Cr:ZnSe medium possesses sufficient optical gain, it is tolerable to additional nonsaturable losses coming from the GSA. To date, acousto-optically mode-locked, SESAM mode-locked, and Kerr-lens mode-locked operation of Cr:ZnSe lasers have been reported [16–18].

In this Letter, we report femtosecond pulse generation from a Cr:ZnSe laser passively mode-locked with high-quality monolayer graphene coated on a CaF_2 substrate. The laser produced a stable train of 226 fs pulses at 2.5 μm with a pulse repetition rate of 77 MHz and average power of 80 mW. The corresponding spectral bandwidth was 37 nm, giving a time–bandwidth product of 0.39. To our knowledge, this represents the longest laser wavelength where graphene was employed as a saturable absorber for mode-locking.

The saturable absorber based on high-quality monolayer graphene was fabricated by employing a similar method described in [8]. The monolayer graphene was synthesized on a Cu film by a chemical vapor deposition technique. After rapid cooling, PMMA was deposited on the grown graphene as a supporting material. The graphene/PMMA layer was then separated from the Cu film by wet etching and transferred onto a CaF_2 substrate of 1 in. diameter. Subsequently, the PMMA was completely removed by using acetone.

As can be seen from the optical transmission curve displayed in Fig. 1, the monolayer graphene shows the zero bandgap behavior with a nearly constant absorption of ≅2.3% above 900 nm up to the mid-infrared spectral region. The amount of absorption is in very good agreement with the theoretically expected value of $\pi\alpha$ for graphene.

Information regarding the quality and number of graphene layers can be inferred from Raman spectrum measurements [19]. Figure 2 shows the Raman spectrum of our sample measured with a Renishaw inVia Raman microscope at the pump wavelength of 532 nm. The well-known D, G, G*, and G′ (2D) bands were clearly observed as expected. From the measured spectrum, the estimated value of the $I_G/I_{G'}$ ratio and the linewidth of the G′ band came to 0.36 and 33 cm^{-1}, suggesting that the transferred graphene was nearly a monoatomic layer. Similar values were reported for monolayer graphene on other substrates in previous studies [20]. In addition, the I_D/I_G ratio is well below 0.3, indicating that the layer is nearly defect free.

Figure 3 shows a schematic of the laser setup used in the mode-locking experiments. A 2.4 mm long Cr:ZnSe crystal was positioned between two highly reflecting concave mirrors (radius of curvature, $ROC = 100$ mm) at Brewster's angle and was water-cooled at 21°C. The crystal was pumped with a 5 W Tm:fiber laser (IPG Photonics, TLR-5-1800-LP) operating at 1.8 μm. The high reflector (HR) and output coupler (OC) arm lengths were 62 and 120 cm, respectively, resulting in a total cavity length of around 2 m. Two Brewster cut CaF_2 prisms (P1 and P2) were placed at minimum deviation in the HR arm for dispersion compensation. The GSA was put at Brewster's incidence between two curved mirrors (M3 and M4, each with [ROC] = 100 mm).

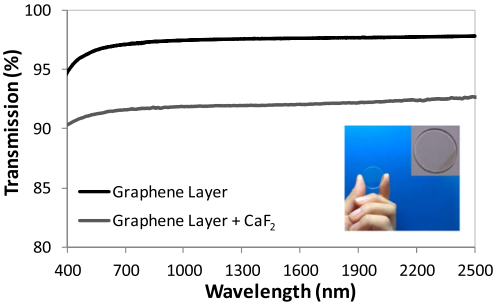

Fig. 1. (Color online) Optical transmission of the high-quality monolayer graphene transferred onto CaF_2.

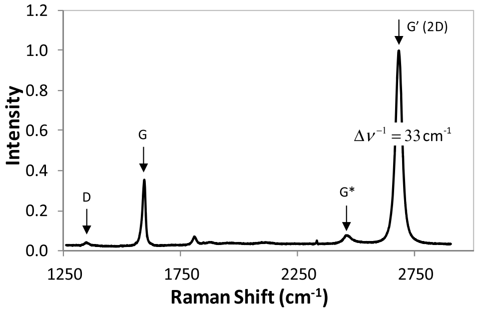

Fig. 2. Measured Raman spectrum of the monolayer graphene on CaF_2.

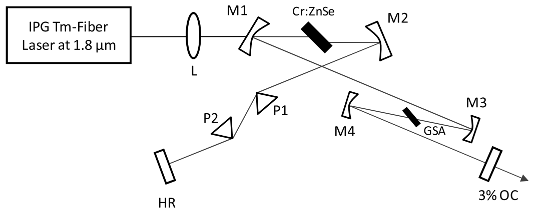

Fig. 3. Experimental setup of the GSA mode-locked Cr:ZnSe laser. M1, M2, M3, and M4 are highly reflecting concave mirrors ($ROC = 100$ mm). L is the pump focusing lens ($f = 7.5$ cm). P1 and P2 are the CaF_2 dispersion compensation prisms.

Figure 4 shows the efficiency curves taken with the Cr:ZnSe laser in different configurations. The laser was operated with a 3% transmitting OC. In the continuous wave (cw) regime, the free-running cavity (without prisms and GSA) produced as high as 300 mW of cw output power at the pump power of 2.3 W. Inclusion of the dispersion compensation prisms, focusing optics (M3 and M4), and the GSA reduced the total output cw power to 120 mW. By comparing the slope of the efficiency curves with that of the empty cavity, the insertion loss of the GSA and focusing optics (M3 and M4) was estimated to be 4.2%. Because the single-pass transmission of GSA at 2500 nm was measured as ~2.1% (see Fig. 1), the estimated round trip passive loss of 4.2% agrees well with the optical transmission data displayed in Fig. 1.

During the mode-locking experiments, we utilized a pair of CaF_2 prisms for dispersion compensation. Taking into account the dispersion of the Cr:ZnSe crystal, prism pair (separation = 22 cm), substrate of GSA (2 mm CaF_2), and insertion of prisms (13 mm CaF_2), the overall group delay dispersion of the cavity was estimated to be $-2609\ \text{fs}^2$. To initiate mode-locking, GSA was translated through the beam waist produced by M3 and M4. Stable mode-locked operation was readily observed and could be sustained for several hours. The minimum output power to initiate mode-locked operation was measured to be 50 mW, when the laser was pumped at 1.1 W (from Fig. 4). Stable, single-pulse mode-locking was obtained up to 80 mW, beyond which cw peaks appeared in the spectrum. Based on a standard ABCD analysis, the estimated spot size on the sample came to 47 μm, which gives a threshold intracavity fluence of 312 $\mu\text{J/cm}^2$ for

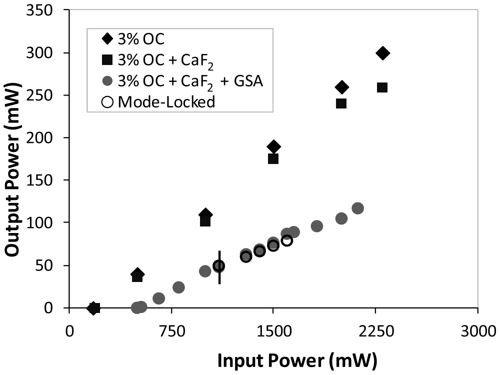

Fig. 4. Efficiency curves of the Cr:ZnSe laser in different configurations.

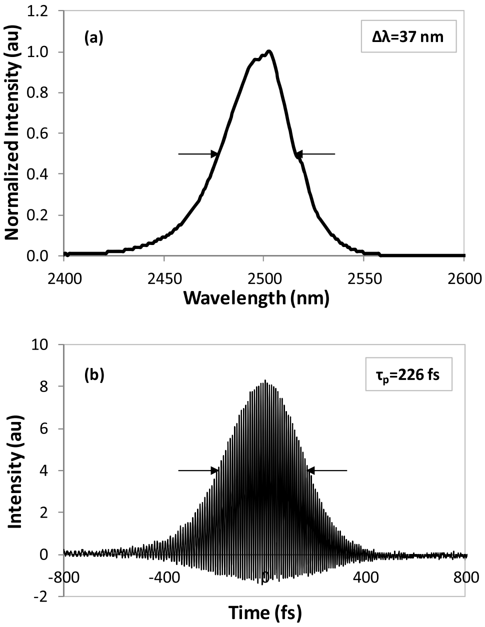

Fig. 5. (a) Measured laser spectrum and (b) measured interferometric autocorrelation trace of the pulses near 2500 nm.

mode-locking at the output power of 50 mW. At the highest mode-locked average output power of 80 mW, the corresponding intracavity fluence on the GSA was determined to be 500 μJ/cm^2. Up to this fluence level, no damage occurred on the surface of the GSA sample. Based on our measurements at other wavelengths above 1000 nm where the linear absorption is nearly constant, we expect a modulation depth of <0.4% and a saturation fluence of <14 μJ/cm^2 for the monolayer GSA near 2500 nm [7].

Figure 5 shows the spectrum and interferometric autocorrelation trace of the generated pulses. The spectrum was measured with a scanning spectrometer. The spectral bandwidth (FWHM) of the pulses was measured to be 37 nm centered around 2500 nm [see Fig. 5(a)]. In the autocorrelation measurements, two-photon absorption in a germanium photo detector was employed [see Fig. 5(b)]. By assuming a sech^2-shaped pulse, the pulse width (FWHM) came to 226 fs with a corresponding time–bandwidth product of 0.39. This is in reasonable agreement with the theoretically expected value of 0.315 for a transform-limited sech^2 pulse.

In conclusion, we demonstrated the operation of a stable 2.5 μm femtosecond Cr:ZnSe laser, passively mode-locked with high-quality, monolayer graphene coated on a CaF$_2$ substrate. The laser produced 226 fs pulses at a repetition rate of 77 MHz with an average power of 80 mW. The measured time–bandwidth product was 0.39. To the best of our knowledge, this represents the first demonstration of a femtosecond Cr:ZnSe laser passively mode-locked with a GSA.

The authors thank Adnan Kurt and Isinsu Baylam for help during the experiments and Baris Yagci for help during the Raman spectrum measurements. This work was supported in part by the National Research Foundation funded by the Korean Government (MEST) (2011-0017494 and 2011-0017587).

References

1. U. Keller, K. J. Weingarten, F. X. Kartner, D. Kopf, B. Braun, I. D. Jung, R. Fluck, C. Hönninger, N. Matuschek, and J. Aus der Au, IEEE J. Sel. Top. Quantum Electron. **2**, 435 (1996).
2. T. Hasan, Z. Sun, F. Wang, F. Bonaccorso, P. H. Tan, A. G. Rozhin, and A. C. Ferrari, Adv. Mater. **21**, 3874 (2009).
3. S. Y. Set, H. Yaguchi, Y. Tanaka, and M. Jablonski, IEEE J. Sel. Top. Quantum Electron. **10**, 137 (2004).
4. I. H. Baek, S. Y. Choi, H. W. Lee, W. B. Cho, V. Petrov, A. Agnesi, V. Pasiskevicius, D. I. Yeom, K. Kim, and F. Rotermund, Opt. Express **19**, 7833 (2011).
5. A. Schmidt, P. Koopmann, G. Huber, P. Fuhrberg, S. Y. Choi, D.-I. Yeom, F. Rotermund, V. Petrov, and U. Griebner, Opt. Express **20**, 5313 (2012).
6. B. V. Cunning, C. L. Brown, and D. Kielpinski, Appl. Phys. Lett. **99**, 261109 (2011).
7. I. H. Baek, H. W. Lee, S. Bae, B. H. Hong, Y. H. Ahn, D.-I. Yeom, and F. Rotermund, Appl. Phys. Express **5**, 032701 (2012).
8. W. B. Cho, J. W. Kim, H. W. Lee, S. Bae, B. H. Hong, S. Y. Choi, I. H. Baek, K. Kim, D.-I. Yeom, and F. Rotermund, Opt. Lett. **36**, 4089 (2011).
9. J. Ma, G. Q. Xie, P. Lv, W. L. Gao, P. Yuan, L. J. Qian, H. H. Yu, H. J. Zhang, J. Y. Wang, and D. Y. Tang, Opt. Lett. **37**, 2085 (2012).
10. F. Bonaccorso, Z. Sun, T. Hasan, and A. C. Ferrari, Nat. Photonics **4**, 611 (2010).
11. Z. Sun, T. Hasan, and A. C. Ferrari, Physica E **44**, 1082 (2012).
12. A. Schliesser, N. Picque, and T. W. Hansch, Nat. Photonics **6**, 440 (2012).
13. H. Xiong, H. Xu, Y. Fu, J. Yao, B. Zeng, W. Chu, Y. Cheng, Z. Xu, E. J. Takahashi, K. Midorikawa, X. Liu, and J. Chen, Opt. Lett. **34**, 1747 (2009).
14. U. Demirbas and A. Sennaroglu, Opt. Lett. **31**, 2293 (2006).
15. E. Sorokin, I. T. Sorokina, M. S. Mirov, V. V. Fedorov, I. S. Moskalev, and S. B. Mirov, in *Advanced Solid-State Photonics* (Optical Society of America, 2010), paper AMC2.
16. T. J. Carrig, G. J. Wagner, A. Sennaroglu, J. Y. Jeong, and C. R. Pollock, Opt. Lett. **25**, 168 (2000).
17. M. N. Cizmeciyan, H. Cankaya, A. Kurt, and A. Sennaroglu, Opt. Lett. **34**, 3056 (2009).
18. I. T. Sorokina, E. Sorokin, and T. Carrig, in *Conference on Lasers and Electro-Optics (CLEO)* (Optical Society of America, 2006), paper CMQ2.
19. A. C. Ferrari, J. C. Meyer, V. Scardaci, C. Casiraghi, M. Lazzeri, F. Mauri, S. Piscanec, D. Jiang, K. S. Novoselov, S. Roth, and A. K. Geim, Phys. Rev. Lett. **97**, 187401 (2006).
20. A. Reina, X. Jia, J. Ho, D. Nezich, H. Son, V. Bulovic, M. S. Dresselhaus, and J. Kong, Nano Lett. **9**, 30 (2008).